Contact and Resume

EQIT-7

Advancing Thermospheric Density Quantification: Applying Energy Dissipation Rate GNSS Accelerometry to the Eccentric C/NOFS Satellite

D. Fitzpatrick[1,2], R. Bishop[2], M. Pilinski[3], S. Palo[1]

[1] Ann and H.J. Smead Department of Aerospace Engineering Sciences, University of Colorado Boulder, Boulder, CO, 80303, United States
[2] Space Science and Applications Laboratory, The Aerospace Corporation, 2310 E. El Segundo Blvd., El Segundo, CA, 90245, United States
[3] Laboratory for Atmospheric and Space Physics, University of Colorado Boulder, Boulder, CO, 80303, United States

AEROSPACE

UNIVERSITY OF COLORADO BOULDER
Ann and H.J. Smead Aerospace Engineering Sciences

LASP

Summary

1. The increase in the number of objects in LEO has heightened the demand for measurements of thermospheric neutral mass density (ND).
2. We develop physics-based "GNSS Accelerometry" methods to quantify ND from spacecraft orbital decay.
3. We provide a framework for applying the physics-based Energy Dissipation Rate method of Sutton et al. (2021) [5] to the eccentric orbit of C/NOFS [1] during Jan. 2011.
4. The merits of the EDR method, especially in its heightened sensitivity to solar/geomagnetic activity, are underscored in a comparative analysis to the TLE-density processing algorithm of Picone et al. (2005) [2] and NRLMSISE-00 [3].
5. The novel application of suborbital-average EDR integration tailored for satellites with eccentric orbits is introduced, offering nuanced insights into thermospheric conditions often obscured by averaging across the entire orbit.

Link to Abstract

Energy Dissipation Rate

1. ✓ Sutton et al. (2021) [5] use satellite ephemerides to calculate the ***Energy Dissipation Rate (EDR)*** and recover neutral density (ND)

EDR Observed Effective Density

$$\rho_{\text{eff}} = \frac{-2m\Delta\xi}{\int_{t_0}^{t_1} C_D A_{\text{ref}} v^3 \text{d}t} = \frac{2m\left(\xi_0 - \xi_1\right)}{\int_{t_0}^{t_1} C_D A_{\text{ref}} v^3 \text{d}t} \quad (3)$$

Non-Spherical Terms

$$^{\mathcal{B}}\Delta\xi = \left[\frac{^{\mathcal{B}}v^2}{2} - \Omega_{\oplus}^2\left(\frac{^{\mathcal{B}}x^2 + {^{\mathcal{B}}y}^2}{2}\right) - \frac{GM_{\oplus}}{r} - U_{g,\mathcal{O}>0}\right]\Bigg|_{t_0}^{t_1} - \int_{t_0}^{t_1} {^{\mathcal{B}}\mathbf{a}_{3B}} \cdot {^{\mathcal{B}}\mathbf{v}}\text{d}t - \int_{t_0}^{t_1} {^{\mathcal{B}}\mathbf{a}_{SRP}} \cdot {^{\mathcal{B}}\mathbf{v}}\text{d}t \quad (4)$$

Tab. 1. EDR variable definitions.

m	Mass	ξ	Specific Energy	C_D	Drag Coefficient
A_{ref}	Cross-Sectional Area	$\mathbf{v}$	Orbital Velocity	$\Omega_{\oplus}$	Earth's Rotation Rate
$r = \sqrt{x^2+y^2+z^2}$	Orbital Radius	$GM_{\oplus}$	Earth's GM	U_g	Gravitational Potential
$\mathcal{O}$	Order	$\mathbf{a}_{3B}$	Third-Body Acceleration	$\mathbf{a}_{SRP}$	SRP Acceleration

2. ✓ UCAR provides POD data [6] for C/NOFS [1]
✓ C_D evaluated using a cylindrical model for C/NOFS as input to SESAM [4]
✓ Eccentricity of C/NOFS requires a careful choice of the integration window (i.e., "orbit arc") to capture a drag signal above the noise floor

3. ✓ For orbit-average ND recovery, each orbit arc is set to span from apoapsis to apoapsis to be nearly centered on the ND local maximum of each orbit

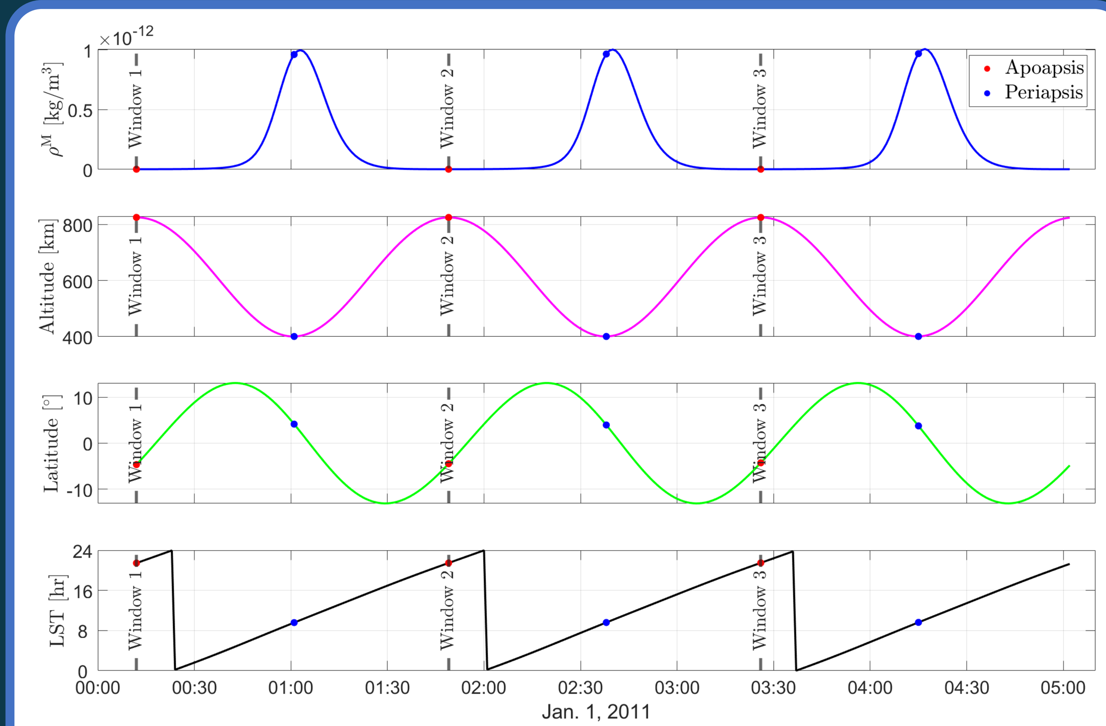

Fig. 1. Time series of NRLMSISE-00 density, geodetic altitude, geodetic latitude, and local solar time for C/NOFS on January 1, 2011 illustrating the apoapsis-to-apoapsis integration windows.

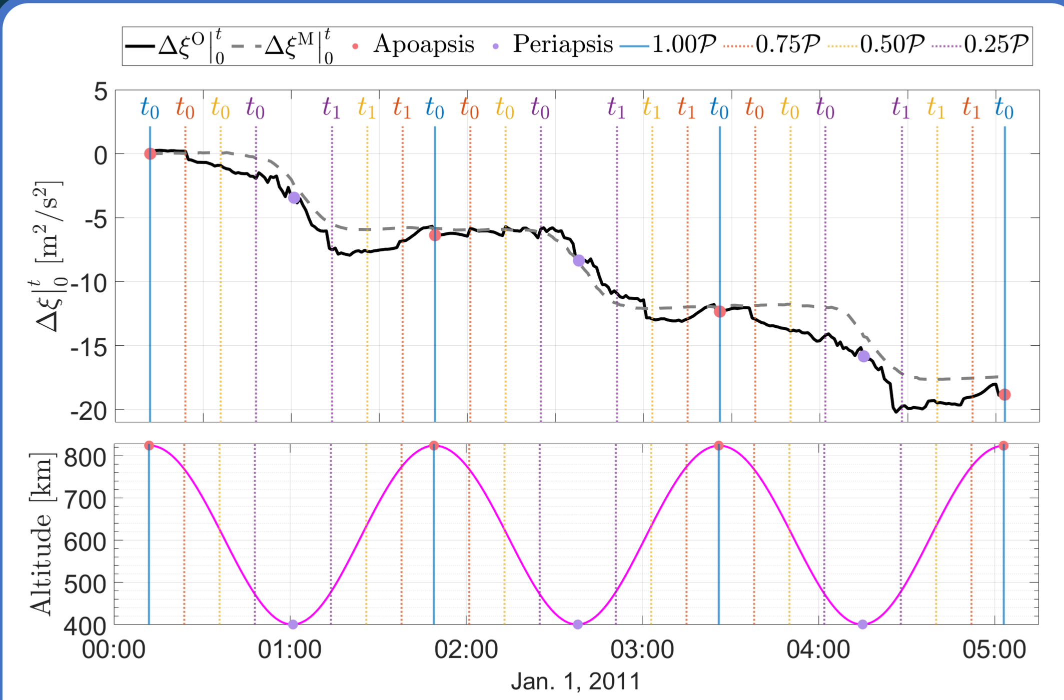

Fig. 2. Time series of (top) observed (UCAR POD; solid line) and modeled (synthetic ODE45; dashed line) C/NOFS orbital energy and (bottom) geodetic altitude illustrating the suborbital integration windows symmetric about periapsis.

4. ✓ For suborbital-average ND recovery (i.e., fractions of an orbital period $\mathcal{P}$), orbit arcs $[t_0, t_1]$ are also nominally centered about periapsis
✓ The eccentricity of C/NOFS results in a greater EDR near periapsis than apoapsis

Orbit-Average: Space Weather Sensitivity

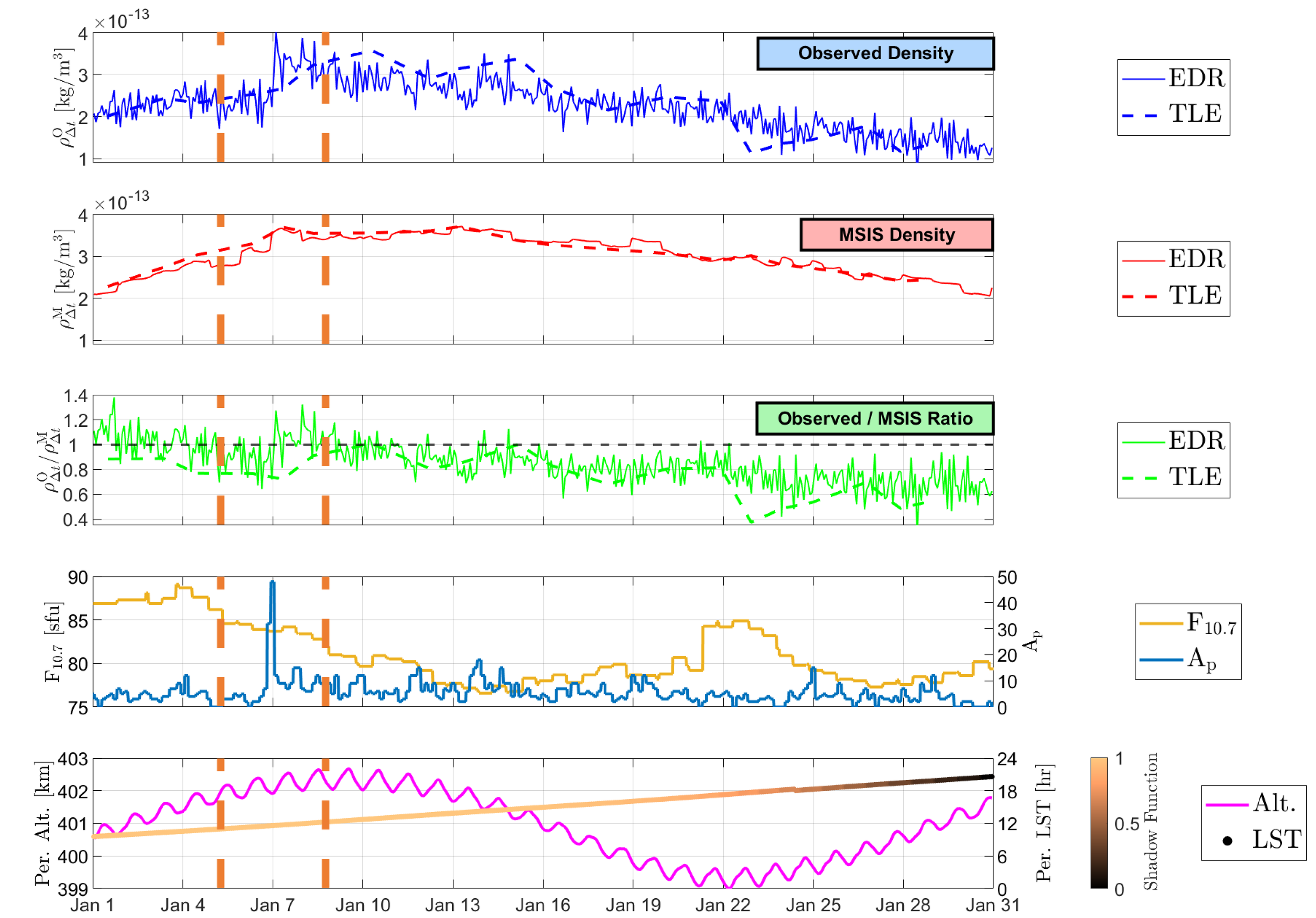

Fig. 3. Time series of observed effective density, model effective density, the ratio between the observed and modeled, A_p and $F_{10.7}$ indices, and periapsis altitude and local solar time. The minor geomagnetic storm on Jan. 7 is highlighted.

1. ✓ EDR and TLE [2] methods exhibit similar trends to each other and are within a [0.3,1.3] factor of NRLMSISE-00 [3]
✓ Ratios being mostly <1 is expected since MSIS runs hot during solar minimum
✓ ***EDR enables identification of minor geomagnetic storm*** better than TLE-method and MSIS
✓ Small-scale variations in the EDR-derived densities are non-physical and may be explained by processing error carried over from the UCAR POD filtering scheme

Suborbital-Average: Nuanced Insights

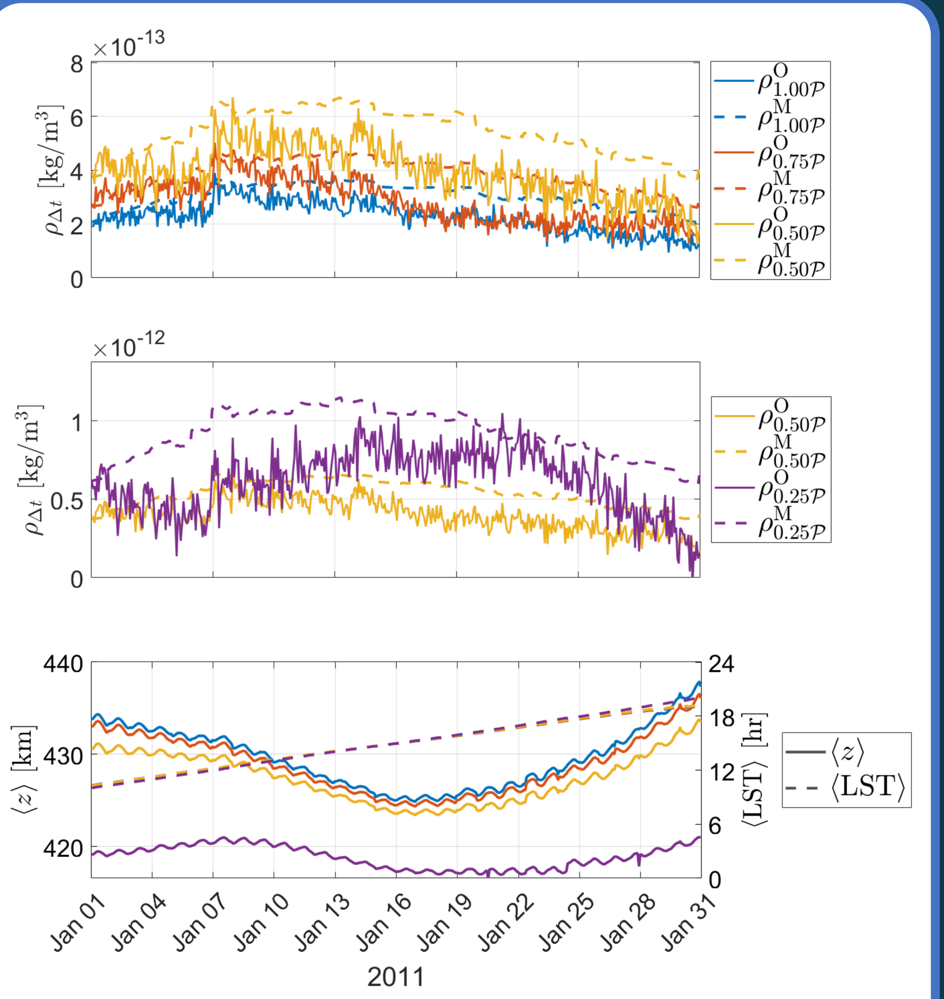

Fig. 4. Time series of C/NOFS (top and middle) observed and modeled densities and (bottom) average window altitude and local solar time for suborbital integration windows of 1.00, 0.75, and 0.50 and 0.25 portions of the duration of an orbital period centered about periapsis.

1. ✓ Suborbital-average integration enables the analysis of specific spatial regions uniquely influenced by defining localized features which can be masked by averaging over the entire orbit
✓ Inverse relationship between arc size and ND magnitude results from the average being weighted more heavily towards the peak density at periapsis
✓ 0.25$\mathcal{P}$ arc underscores a prominent transition in drag SNR
✓ Density inversion and anisotropic behavior seen in 0.25$\mathcal{P}$ arc may be attributed to complications arising from the relative balance of altitude, LST, $F_{10.7}$, and/or additional vertical structures (i.e., planetary waves)

2. ✓ Arcs can also be chosen as two sequential half-orbit arcs: "inbound" (apoapsis to periapsis) and "outbound" (periapsis to apoapsis)
✓ Influence of LST on ND is highlighted by outbound arc's transition from dayside to nightside, absent in inbound arc

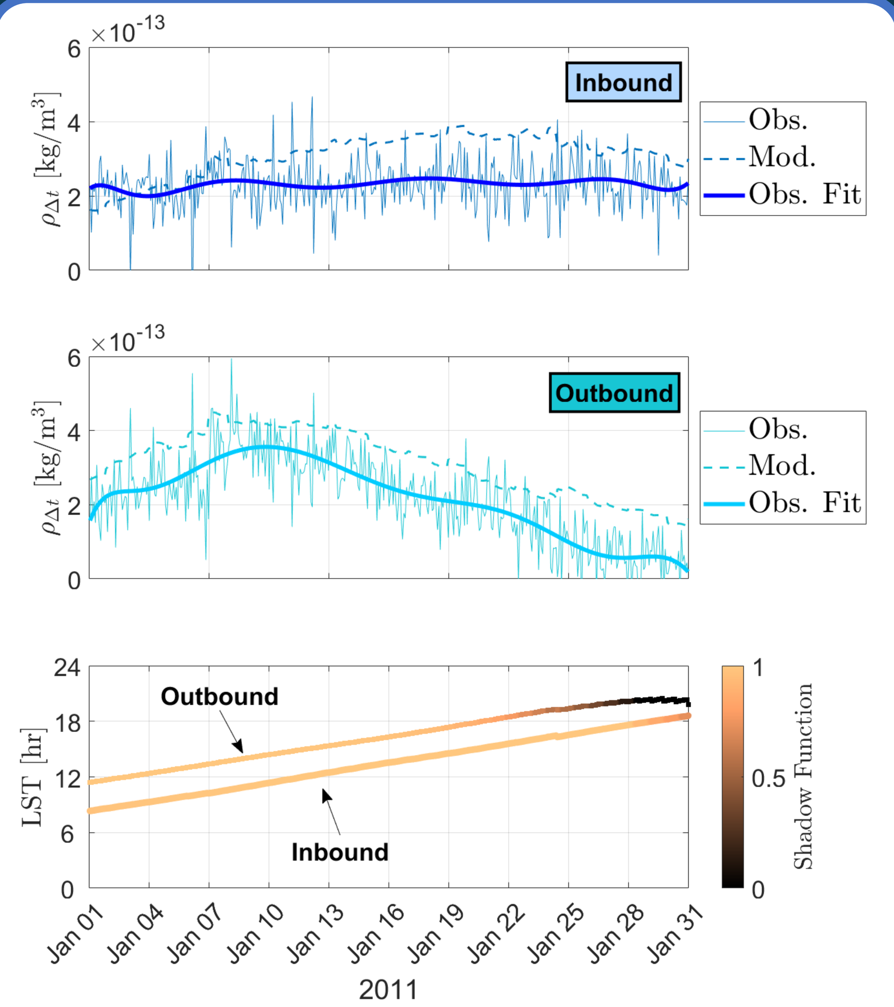

Fig. 5. Time series of (top and middle) observed and model effective densities overlaid with a polynomial fit to the observed data and (bottom) average window local solar time color-mapped to the solar shadow function for the "inbound" (apoapsis to periapsis) and "outbound" (periapsis to apoapsis) half orbits with respect to periapsis.

References and Acknowledgements

[1] de La Beaujardi`ere, O. (2004). C/nofs: a mission to forecast scintillations. Journal of Atmospheric and Solar-Terrestrial Physics, 66 (17), 1573-1591.
[2] Picone, J. M., Emmert, J., & Lean, J. (2005). Thermospheric densities derived from spacecraft orbits: Accurate processing of two-line element sets. Journal of Geophysical Research, 110 , A03301.
[3] Picone, J. M., Hedin, A. E., Drob, D. P., and Aikin, A. C. (2002). NRLMSISE-00 empirical model of the atmosphere: Statistical comparisons and scientific issues, J. Geophys. Res., 107(A12), 1468.
[4] Pilinski, M. (2011). Dynamic gas-surface interaction modeling for satellite aerodynamic computations. PhD thesis, University of Colorado, Boulder, Department of Aerospace Engineering Sciences.
[5] Sutton, E. K., Thayer, J. P., Pilinski, M. D., Mutschler, S. M., Berger, T. E., Nguyen, V., & Masters, D. (2021, 6). Toward accurate physics-based specifications of neutral density using gnss-enabled small satellites. Space Weather , 19.
[6] University Corporation for Atmospheric Research, CDAAC GNSS Radio Occultation Datasets, C/NOFS.

This work was supported by the National Science Foundation (Award Numbers: 1936512, 1936518, 1936537, 1936538, 1936550, and 1936665) and partially supported by The Aerospace Corporation's Technical Investment Program. The authors would also like to thank Dr. Eric Sutton for his contributions.

EDR Derivation